Experimental analysis of density peaking in KSTAR plasma

Cheol-Sik Byun [a], Chanyoung Lee [a] and Yong-Su Na [a*]
[a]*Department of Nuclear Engineering, Seoul National University, Seoul, Korea*
[*]*Corresponding author: ysna@snu.ac.kr*

1. Introduction

In fusion reactor such as ITER, accurate predictions of density peaking are essential due to the strong dependency of fusion power and bootstrap current on the density profile. To predict the density peaking of ITER, various experiments related particle transport have been conducted in present devices. Previous studies found the inverse-proportional trend of density peaking in terms of the effective collision frequency through experimental observations in ASDEX Upgrade [1, 2], JET [3, 4], Alcator C-MOD [5] and JT-60U [6]. In this study, we attempted to reproduce the inverse-proportional trend of the multi-devices in KSTAR experiments with interpretative simulations for more rigorous understanding.

2. Methods

In this section, assumptions and techniques to decide the representative value of density peaking in a discharge in KSTAR are described. Also, flexible integrated suite of code, TRIASIC [7] which is newly developed for exploiting merits of the standardized data model, IMAS for interpretative simulation in KSTAR is introduced.

2.1 KSTAR database for analysis of density peaking

For the physical analysis, discharges should have profile data of electron density and temperature from Thomson diagnostics, ion temperature and rotating velocity from CES diagnostics. The target time for analyzing should be chosen seriously as MHD instabilities such as sawtooth and ELM can change engineering parameters including electron density profile rapidly. The density peaking factor is fluctuated as shown in Fig. 1.

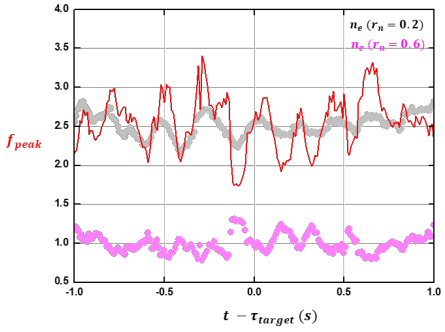

Fig. 1. Experimental data for density peaking factor. Density value in $r_n = 0.2$ (gray dot) and in $r_n = 0.6$ (magenta dot). The peaking factor, where $f_{peak} = n_e(r_n = 0.2)/n_e(r_n = 0.6)$ (red line)

For selecting the representative value of peaking factor, averaged Thomson data is used and the target time is chosen without ELM instabilities.

2.2 Integrated simulator, TRIASIC (Tokamak Reactor Integrated Automated Suite for Simulation and Computation)

Physical values were calculated from experimental engineering parameters through integrated simulator, TRIASIC. This suite has various modules of core transport solver such as ASTRA and C2, equilibrium solver such as CHEASE, transport model such as TGLF, NEO, NCLASS and H&CD model such as NUBEAM, TORAY and CURRAY. By appropriate combination of each module, various purpose of predictive/interpretative analysis can be done. The validity of this suite was successfully confirmed in about 50 stationary discharges of various KSTAR scenarios [7].

3. Results

3.1 Inverse-proportional trend of density peaking in terms of effective collision frequency in KSTAR

In previous studies, experimental research has been intensively dedicated to the identification of the mechanisms which underlie the density profile peaking and on its scaling with various local plasma parameters. Statistical analyses of the experimental databases have shown that collision frequency was indeed the parameter which has the largest bivariate correlation with density peaking as well as the largest statistical significance and statistical relevance in regression [8]. They showed that density peaking is inverse proportional to the effective collision frequency, where

$$\nu_{eff} \equiv \nu_{ei}/\omega_{DE} \sim 2Z_{eff} < n_e > / < T_e >^2 \quad (1)$$

From KSTAR experiments database, we successfully reproduced the previous observations in ASDEX Upgrade, JET, Alcator C-MOD, and JT-60U as shown in Figure 2. Comparing with the result of other devices, it has broader scatter. Because all kinds of KSTAR discharges are plotted, while discharges of the typical H-mode are plotted in the previous studies. For the analyzing the effects of each parameter, the deconstructing scatter of Fig. 2 is necessary. But it was hard to understand each effect separately because each point has multi-dimensional engineering parameters which are strongly correlated each other.

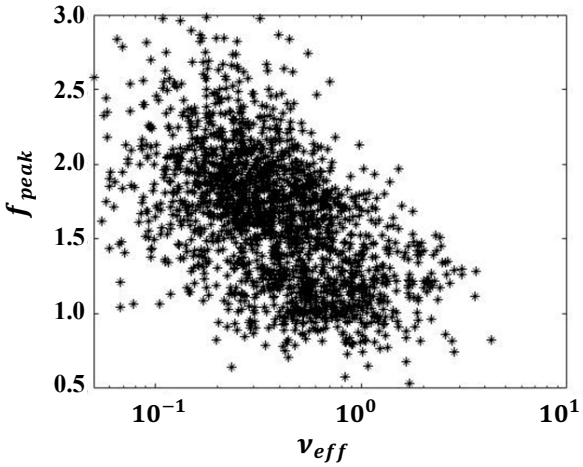

Fig. 2. Density peaking as a function of the effective collision frequency in KSTAR discharges

3.2 Distinct deviation of the inverse-proportional trend in terms of effective collision frequency in KSTAR

A distinct deviation of the inverse proportional trend has been identified for discharges with NB-C and B in 2018 year as shown in Fig. 3. KSTAR has three beam A, B, and C. Among three beams, NB-C is the most perpendicular and absorption length is the shortest. Comparing with discharges with NB-A and B, density profile of discharges with NB-C and B is less peaked in the same effective collision frequency. However, the inverse proportional trend between density peaking and effective collision frequency is kept though the degree of inverse proportion is decreased.

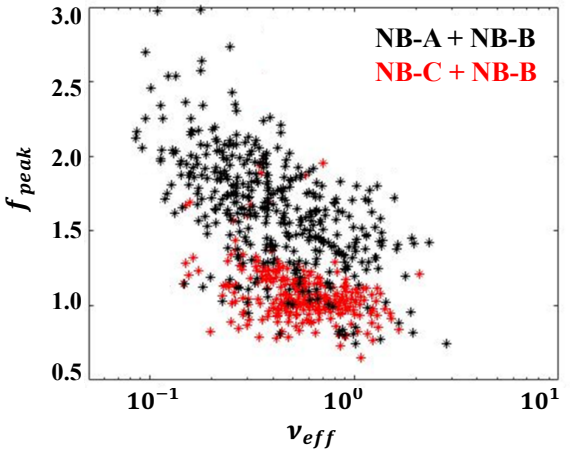

Fig. 3. Density peaking as a function of the effective collision frequency in 2018 KSTAR discharges with combination of NB-A and B (black) and combination of NB-C and B (red).

4. Discussion

Density peaking factor is decided by the balance of diffusion, particle pinch, source, and loss in the particle transport. As the difference of NB combination make the trend deviation, we supposed particle pinch or source is the main cause of this phenomenon. As the neoclassical pinch is negligible in low collisionality plasma, the particle pinch in here means the anomalous pinch such as curvature and thermo diffusive pinch. If the turbulence is stabilized, the value of anomalous pinch could be decrease. And the density peaking is also decreased because the anomalous pinch usually directs inward. The first and second candidates are turbulence stabilizing factor and they can change largely with the combinations of NBI. The last candidate is related to the source.

In this section, the possible candidates for the deviation of inverse-proportional trend as shown in Fig. 3 are introduced. The first and second candidates are turbulence stabilizing factor and they can be changed largely with NB combination. The last candidate is related to the source with NB fueling.

4.1 Turbulence stabilizing - Rotational shear effect

The significant suppression of Ion Temperature Gradient (ITG) dominated plasma turbulence via electro-magnetic fluctuations and fast ions, for instance, has opened up the scope of turbulence reduction by alternative mechanisms to the well-known $E \times B$ shearing [10]. As NB-C is the most perpendicular beam, it can be expected that discharges with combination of NB-C and B have lower toroidal velocity as shown in Fig. 4 (a). However, the shear of toroidal velocity is similar as shown in Fig. 4 (b). As the important thing to stabilize turbulence is the rotation shear, it would be hard to say the rotation shear is the main cause of deviation.

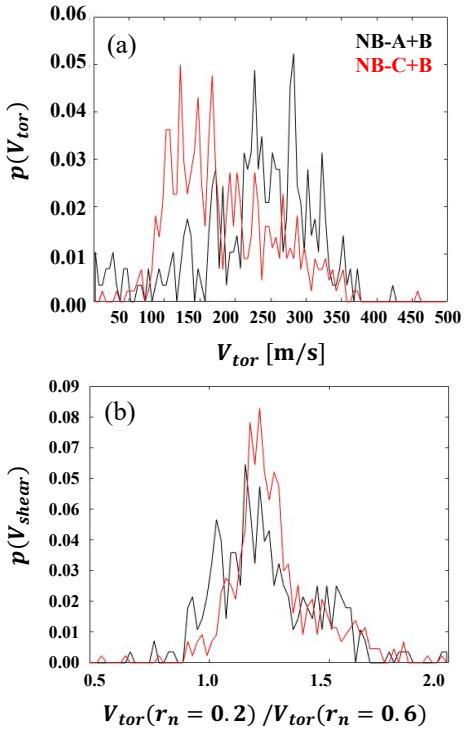

Fig. 4. Probability distribution of toroidal velocity (a) and shear of toroidal velocity (b) in 2018 KSTAR discharges with

combination of NB-A and B (black) and combination of NB-C and B (red)

4.2 Turbulence stabilizing – fast particle effect

Recent study shows that fast ions have a stabilizing influence on the ITG mode and reduces the peaking of the main ion and electron density profiles. The simulation result without considering fast ions has higher density gradient length which make the ion flux zero than those with considering fast ions [11]. As KSTAR operated in low density condition ($\overline{n_e}$~$0.7 - 1.5\ [m^{-3}]$) in 2018 year, the perpendicular beam should be lower beam energy as can be seen in Figure 5. Lower beam energy could increase the cross-section and absorption rate, which make density of fast ion increase. However, the various researches are needed to confirm this hypothesis.

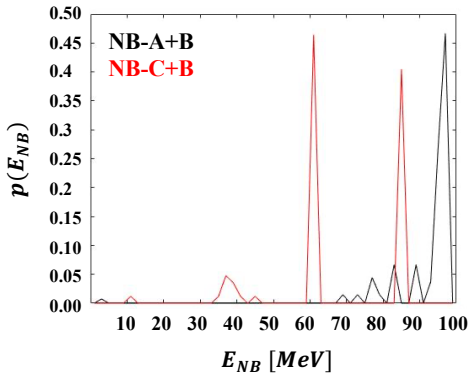

Fig. 5. Probability distribution of energy of NB-A in 2018 KSTAR discharges with combination of NB-A and B (black) and combination of NB-C and B (red)

4.3 Source – NB fueling effect

NB fueling can make the trend deviation as well as the anomalous pinch. To separate fueling effect, the reference discharges are chosen in Fig. 3 with same condition such as ν_{eff}~$0.46, q_{95}$~$5.0, \overline{n_e}$~$5.25 \times 10^{19}\ [m^{-3}]$ and P_{NB}~$2.9\ [MW]$. But they have different combination of NB and the value of density peaking factor. #21571 represents 2018 discharge with combination of NB-A and B and #20949 represents 2018 discharge with combination of NB-C and B. Density peaking factor of #20949 and #21571 is 1.217 and 1.469, respectively. The density profile of fast particle was calculated by using NUBEAM in TRIASIC. As shown in Fig. 6, #20949 has broader source distribution than #21571.

Although the non-linear transport calculations are essential for more rigorous analysis, the contribution of NB fueling on the density peaking is obvious. As ITER will have low NB fueling comparing with present-devices, the density profile of ITER could be flatter than expected by empirical scaling in the previous studies.

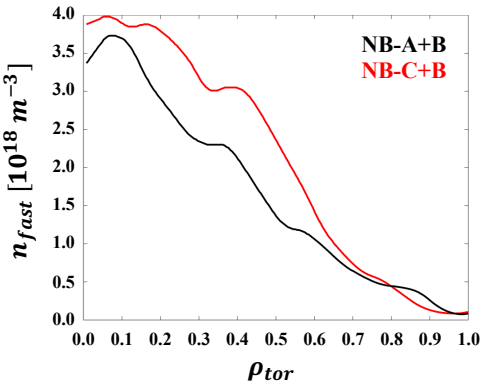

Fig. 6. Source distribution calculated by NUBEAM in #21571 (black) and #20949 (red).

4. Conclusion

Overall exploration of the density peaking for KSTAR experiments is conducted. The inverse-proportional trends of the density peaking in terms of effective collision frequency is reproduced. And the distinct deviation of the trend has been identified for 2018 KSTAR discharges with combination of NB-B and C. We supposed that the causes of this finding are the stabilizing turbulence effect and source effect. As the rotation shear is similar, the rotation shear for stabilizing turbulence may not be the main cause. Other candidate of the stabilizing turbulence effect is the fast ions. We could check recent study about effect of fast ions on density peaking based on KSTAR experiment. Lastly, the NB fueling is identified obviously as cause of the trend deviation by source modeling. To classify the exact portion of contribution for each effect, the non-linear transport simulation including fast ion is planned as future works.

REFERENCES

[1] Angioni C et al, Density Peaking, Anomalous Pinch, and Collisionality in Tokamak Plasmas, Phys. Rev. Lett., Vol. 90, Article no. 205003, 2003.
[2] Angioni C et al, Theory-based modeling of particle transport in ASDEX Upgrade H-mode plasmas, density peaking, anomalous pinch and collisionality, Phys. Plasmas, Vol. 10, Article no. 3225, 2003.
[3] Weisen H et al, Collisionality and shear dependences of density peaking in JET and extrapolation to ITER, Nucl. Fusion, Vol. 45, No. 2, Article no. L1, 2005.
[4] Weisen H et al, Scaling of density peaking in JET H-modes and implications for ITER, Plasma Phys. Control. Fusion, Vol. 48, Article no. A457, 2006.
[5] Greenwald M et al, Density profile peaking in low collisionality H-modes: comparison of Alcator C-Mod data to ASDEX Upgrade/JET scalings, Nucl. Fusion, Vol. 47, Article no. L26, 2007.
[6] Takenaga H et al, Comparisons of density profiles in JT-60U tokamak and LHD helical plasmas with low collisionality, Nucl. Fusion, Vol 48, No. 7, Article no. 075004, 2008.
[7] Chanyoung Lee et al, Development of Integrated Suite of Codes and Its Validation on KSTAR, 28th IAEA Fusion Energy Conference, May. 10-15, 2021, Nice, France.

[8] Angioni C et al, Particle transport in tokamak plasmas, theory and experiment, Plasma Phys. Control. Fusion, Vol. 51, Article no. 124017, 2009.
[9] Hoang G T et al, Parametric Dependence of Turbulent Particle Transport in Tore Supra Plasmas, Phys. Rev. Lett., Vol. 93, Article no. 135003, 2004.
[10] Garcia J et al, A new mechanism for increasing density peaking in tokamaks: improvement of the inward particle pinch with edge $E \times B$ shearing, Plasma Phys. Control. Fusion, Vol. 61, Article no. 104002, 2019.
[11] Eriksson F et al, Impact of fast ions on density peaking in JET: fluid and gyrokinetic modeling, Plasma Phys. Control. Fusion, Vol. 61, Article no. 075008, 2019.